

Photodissociation of the *tert*-butyl Radical, C₄H₉[†]

M. Zierhut, W. Roth, and I. Fischer*

Institute of Physical Chemistry, University of Würzburg, Am Hubland, D-97074 Würzburg, Germany

Received: March 18, 2004; In Final Form: April 23, 2004

We report results on the photodissociation dynamics of the *tert*-butyl radical, C₄H₉. A beam of internally cold radicals is generated by supersonic jet flash pyrolysis of azo-*t*-butane. Upon optical excitation, the radical dissociates into 2-methylpropene (iso-butene) and a hydrogen atom that is detected by time-resolved photoionization. By varying the excitation wavelength between 355 and 266 nm, unimolecular dissociation rates are obtained as a function of excitation energy. Whereas at low excitation energies, the rates are on the order of 10⁸ s⁻¹, in agreement with simple RRKM calculations. However, the reaction slows down at excitation wavelengths shorter than 329 nm. The data are discussed in light of previous results on the ethyl radical.

Introduction

Alkyl radicals play a key role as reactive intermediates in chemical reactions, in particular in combustion processes and hydrocarbon cracking.¹ Since knowledge of the reaction kinetics is necessary for modeling such reactions,² there is considerable interest in elucidating the dissociation dynamics of isolated radicals. The most important unimolecular reaction channel in many radicals is the loss of a hydrogen atom and formation of a closed shell molecule. In the case of *tert*-butyl, the molecular product formed upon H-atom loss will be 2-methyl-1-propene (iso-butene). The heat of reaction $\Delta_R H^\circ$ for i-C₄H₈ + H relative to *tert*-butyl is 152 ± 3 kJ/mol. The value is based on a heat of formation $\Delta_f H^\circ = 48 \pm 3$ kJ/mol for the *tert*-butyl radical and $\Delta_f H^\circ = -17.9 \pm 1.1$ kJ/mol for iso-butene.³ Since a reverse barrier of around 6 kJ/mol was extrapolated for the reaction,⁴ we expect an activation energy of roughly 158 kJ/mol for hydrogen loss from *tert*-butyl.

In a series of papers, we investigated the unimolecular dissociation of allyl,^{5–7} propargyl,⁸ and ethyl⁹ radicals by depositing sufficient energy for dissociation by optical excitation. The dissociation dynamics and kinetics were then studied by time-resolved detection of H-atoms and by Doppler spectroscopy.¹⁰ The detection of hydrogen atoms by Lyman- α radiation was shown to be a sensitive tool for the observation of radical reactions. However, the interpretation of the results within statistical theories of chemical reactions, i.e., treatment as a thermal reaction of a microcanonical ensemble, relies on a conversion of electronic energy into internal energy that is fast compared to the dissociation rate. At least for the ethyl radical, C₂H₅, this assumption has to be questioned, because the observed dissociation rates were 3–4 orders of magnitude lower than expected from simple RRKM calculations.⁹ This discrepancy motivated us to carry out experiments on larger alkyl radicals in order to get more insight into their photodissociation dynamics. In this paper, we thus report experiments on the photodissociation dynamics of the *tert*-butyl radical, C₄H₉, yielding rates for the unimolecular dissociation to iso-butene and a hydrogen atom.

The UV spectrum of the *tert*-butyl radical shows several well separated absorption bands.¹¹ The first band, corresponding to excitation from the X ²A₁ ground state to the ²A₁ (3s) Rydberg state, extends from 360 to 300 nm and is centered around 333 nm. The transition into the 3p band, comprising a ²A₁ and a ²E state is centered around 253 nm. The strongest UV band corresponds to excitation of another ²A₁ (3d) state and is centered around 233 nm. All assignments were confirmed by ab initio computations.¹² Like in other alkyl radicals, all three bands are broad and featureless; thus, a fast internal conversion to the electronic ground state as the initial process following photoexcitation was suggested to explain the diffuse appearance of the spectra. Note that all bands in *tert*-butyl are significantly red-shifted as compared to ethyl. In C₂H₅, absorption to the ²A' (3s) state peaks around 250 nm. The 3p bands are centered around 204 nm and thus not easily experimentally accessible. Therefore, the *tert*-butyl radical provides the opportunity to study the photodissociation of an alkyl radical over a rather large energy range. Below we will describe experiments performed between 355 and 266 nm (337–450 kJ/mol), corresponding to excess energies in the range between 185 and 298 kJ/mol.

Experimental Section

All experiments were carried out in a differentially pumped standard molecular beam apparatus, equipped with a 0.5 m time-of-flight mass spectrometer. A molecular beam of internally cold *tert*-butyl radicals was produced by supersonic jet flash pyrolysis of azo-*t*-butane, commercially obtained from Aldrich and used without further purification, seeded in 1.0 bar of argon. The details of the design of our pyrolysis nozzle are described elsewhere.¹³ The radical beam passes through a skimmer into the main chamber, where it is crossed by two counterpropagating laser beams: one for excitation of the *tert*-butyl radical and one for the detection of the hydrogen atoms.

Hydrogen atoms were detected by multiphoton ionization.¹⁴ The output of a dye laser (Sirah Precision Scan, operating with pyridine 2) pumped by a Nd:YAG laser (Spectra Physics LAB 170) was frequency doubled in a KDP crystal, producing around 10 mJ at 365 nm, and focused by a 150 mm lens into a cell filled with 50 mbar of Krypton in order to produce VUV radiation around 121.6 nm (Lyman- α). Since the bandwidth of the fundamental is around 0.1 cm⁻¹, we estimate a bandwidth

[†] Part of the special issue "Richard Bersohn Memorial Issue".

* To whom correspondence should be addressed. E-mail: ingo@phys-chemie.uni-wuerzburg.de.

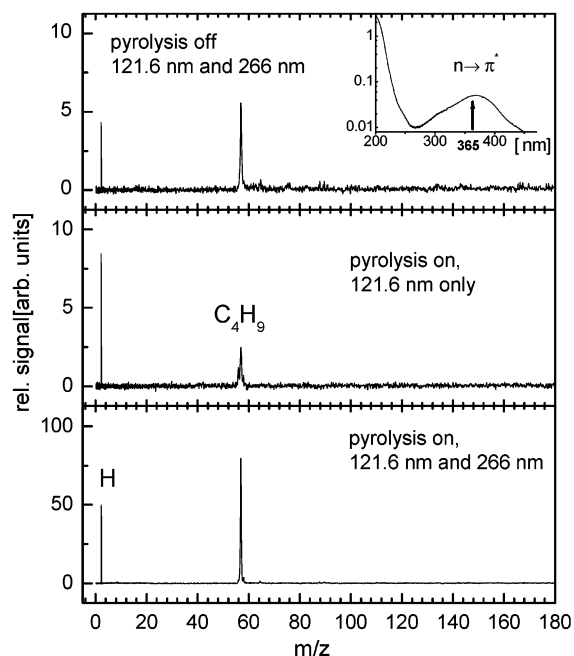


Figure 1. Typical mass spectra of azo-*t*-butane; top trace: Even without pyrolysis almost no signal at the mass of the precursor ($m/z = 142$) is detected because of photodissociation by the residual 365 nm radiation (inset of top trace: absorption spectrum of the precursor). Center trace: With pyrolysis on and only the 121.6 nm detection laser present, a certain amount of hydrogen atoms is detected. Bottom trace: When the 266 nm excitation laser is turned on, a strong H-atom signal emerges. Note the different scales on the y axis for ease of viewing.

of 0.3 cm^{-1} for the VUV pulse. The VUV light was focused into the ionization region by a 100 mm MgF_2 lens mounted at the exit of the cell. Absorption of 121.6 nm radiation excites hydrogen atoms from the 2S ground state to the 2P state and the residual fundamental ionizes the excited atoms, which are subsequently detected in a Wiley–McLaren time-of-flight spectrometer. Fields of 300 and 1000 V/cm were employed in the two acceleration regions. The ions were detected by a single-stage microsphere plate detector (El Mul technology). The signals were recorded in a digital storage oscilloscope, averaged over typically 200 shots, and transferred to a computer.

For excitation of the radicals either the third and fourth harmonic of a YAG laser (Continuum SL I-10) or the frequency-doubled output of another dye laser (Spectra Physics PDL 2, operating with DCM in DMSO) pumped by this Nd:YAG laser were used. The output pulse of the Continuum YAG laser was stretched to approximately 9 ns to achieve stable operation of the Littrow-design dye laser with its relatively long cavity. Typically, 2–3 mJ of the unfocused laser light were employed for excitation. The two laser systems were synchronized externally by using digital delay generators (Stanford Research DG535) to within better than 2 ns.

To optimize our setup, we performed control experiments on cycloheptatriene (CHT), which yielded a rate constant of $3.8 \times 10^6 \text{ s}^{-1}$ for hydrogen loss upon 266 nm excitation, a factor of 1.5 slower than the rate of $(2.6 \pm 0.5) \times 10^6 \text{ s}^{-1}$ published for 248 nm excitation.¹⁵

Results

(a) Mass Spectra. In Figure 1, typical mass spectra relevant for our conditions are presented. Note that different scales for the y axis were employed in the different spectra for ease of viewing. With the pyrolysis source turned off and both excitation

(266 nm) and detection (121.6 nm) lasers present (top trace), almost no signal of the precursor azo-*t*-butane ($m/z = 142$) is detected. Instead, signals at $m/z = 57$, the mass of *tert*-butyl radical, and $m/z = 1$, a hydrogen atom, appear. This behavior is presumably due to photodissociation of the precursor: In the inset of the top trace, the gas-phase absorption spectrum of azo-*t*-butane is shown, recorded at 298 K in a UV/vis spectrometer (Perkin-Elmer Lambda 19, 5 mm beam path). It displays a broad band between 260 and 450 nm, maximizing just around 365 nm, which is attributed to the $n-\pi^*$ transition.¹⁶ Thus absorption of the residual 365 nm radiation employed to generate the VUV light leads to efficient fragmentation of azo-*t*-butane and formation of *tert*-butyl radicals. The 266 nm light leads to some photodissociation of the radical and produces a small H-atom background. Note that these photolytically produced radicals are internally hot, whereas pyrolytically produced radicals are cooled in the supersonic expansion.

When the pyrolysis source is turned on, and only the detection laser at 121.6 nm is present (center trace), a signal at mass 1 is detected, either due to H-atoms formed in the pyrolysis source or, less likely, by 121.6 nm photodissociation. When the excitation laser (266 nm) is turned on, the intensity of the *tert*-butyl and the hydrogen atom signal increases dramatically (bottom trace). The magnitude of the H-atom signal depended linearly on the excitation laser energy at all wavelengths, verifying that only a one-photon process takes place. The detection laser was delayed by 100 ns with respect to the excitation laser. The mass spectra recorded in the 320–355 nm range were similar in appearance; however, the magnitude of the two-color signal was significantly smaller, due to the smaller absorption cross section.

Since a background due to H-atoms formed in the pyrolysis source and due to radicals formed by photodissociation of the unpyrolyzed precursor was present, we carried out numerous control experiments with the pyrolysis source turned off. The background signal obtained without the excitation laser was subtracted when necessary.

(b) Time Delay Scans. To obtain microcanonical rates for the hydrogen loss, the H-atom signal was monitored as a function of the time delay between the excitation and the detection laser. Such time-delay scans were recorded at several wavelengths between 320 and 340 nm and at 266 and 355 nm, respectively. Figure 2 shows by way of example three time-delay scans at 330 nm (top trace), 325 nm (center trace), and 266 nm (bottom trace). The hydrogen signal shows a fast rise time, a short plateau, and a decay at longer delay times. A large difference is evident: At 330 nm, the signal shows a very fast rise, reaching the maximum value around 30 ns, whereas at 325 nm and at 266 nm, the plateau is reached after 60–80 ns only. Rate constants were extracted from the curves by using the following expression¹⁷ to describe the time dependence of the hydrogen signal $S_H(t)$:

$$S_H(t) = N[e^{-k_2 t} - e^{-k_H t}] \quad (1)$$

Here k_H is the unimolecular rate constant for hydrogen loss from *tert*-butyl and k_2 accounts for the decay of the signal. The decay is due to the motion of the hydrogen atoms out of the detection region. It is determined by the experimental conditions and does not have any physical significance. From eq 1, we derived rate constants of $k_H = 1.1 \pm 0.1 \times 10^8 \text{ s}^{-1}$ for 330 nm excitation, $k_H = 2.7 \pm 0.7 \times 10^7 \text{ s}^{-1}$ for 325 nm, and $k_H = 2.8 \pm 0.4 \times 10^7 \text{ s}^{-1}$ for 266 nm excitation. Thus, surprisingly, the rate for H-loss from *tert*-butyl decreases upon increasing the excitation energy from 330 to 325 nm.

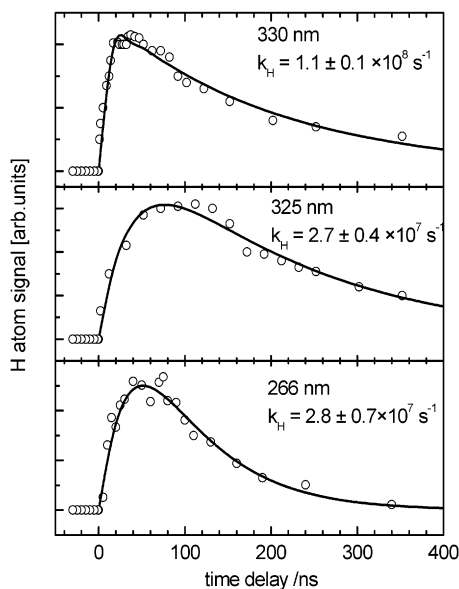


Figure 2. Typical time-delay scans recorded at excitation wavelengths of 330 nm (top trace), 325 nm (center trace), and 266 nm (bottom trace) excitation.

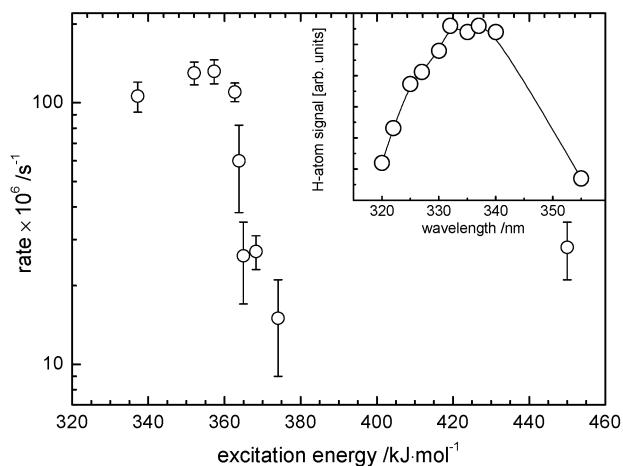


Figure 3. Dissociation rate as a function of excitation energy. A fast rate k_H on the order of $1 \times 10^8 \text{ s}^{-1}$ is measured at excitation energies between 335 and 360 kJ/mol (80 and 87 kcal/mol). Slower rates are measured at higher excitation energies. The H-atom action spectrum shown in the inset matches the published absorption spectrum.

Since nanosecond lasers were used, a rate constant on the order of $1 \times 10^8 \text{ s}^{-1}$ is close to the experimental limit. However, this rate corresponds to a signal that reaches its maximum in 20–30 ns. When the excitation laser power at 266 nm was increased significantly, we observed a very fast rising H-atom signal due to multiphoton excitation that reached its maximum within 10 ns, limited by the laser cross correlation and yielding a rate constant larger by a factor of 2. Thus, we believe that the rates reported here are reliable. Rates were also measured at numerous other wavelengths. In Figure 3, all rates measured are depicted as a function of excitation energy. At selected energies, repeated scans were recorded, as reflected in the error bars of the data points. Interestingly, a sudden step becomes visible at excitation energies between 360 and 375 kJ/mol (329–325 nm), corresponding to excess energies of $\approx 200 \text{ kJ/mol}$ and more. At an excitation wavelength above 330 nm, the observed rates are on the order of $k_H = 1 \times 10^8 \text{ s}^{-1}$, and at shorter wavelengths, the rates drop by an order of magnitude to $k_H = 1\text{--}3 \times 10^7 \text{ s}^{-1}$. The value obtained for excitation at 266 nm (450 kJ/mol) into the 3p state is on the same order of magnitude.

To test whether the rates are in agreement with the expectations from statistical theory, we performed RRKM calculations for the unimolecular dissociation of the *tert*-butyl radical. All frequencies, for *tert*-butyl and the transition state, were taken from the literature.^{18,4} An activation energy $E_A = 158 \text{ kJ/mol}$ (37.8 kcal/mol) was assumed. A difficulty in the *tert*-butyl radical is the presence of several hindered methyl rotors that has to be taken into account, three in the radical and two in the transition state. In our calculations, we used vibrational wavenumbers of 10, 50, and 100 cm^{-1} for the rotors to mimic the behavior of the methyl rotors without taking the internal rotation into account explicitly and assumed a reaction path degeneracy of three. Note that the reaction path degeneracy is nine, when the methyl torsions are treated as free rotors.¹⁹ We calculated rates using two different programs, one employing direct state count²⁰ and the other one utilizing the Whitten-Rabinovich algorithm,²¹ both yielding very similar results. For the H-atom loss from *tert*-butyl at 355 nm (337 kJ/mol), a rate constant of $2.2 \times 10^9 \text{ s}^{-1}$ was calculated using 100 cm^{-1} for the rotors and $1.0 \times 10^9 \text{ s}^{-1}$ using 50 cm^{-1} . At 330 nm, rates are expected to be roughly a factor of 2 faster. Taking the simplicity of the model into account, the fast rates observed between 355 and 330 nm are in reasonable agreement with the rates expected from RRKM calculations. At an excitation wavelength of 320 nm, we calculate a rate of $3.0 \times 10^9 \text{ s}^{-1}$ using 50 cm^{-1} for the rotors, more than 2 orders of magnitude faster than experimentally observed. Rates at 266 nm are calculated to be faster by another factor of 5 as compared to the rate at 320 nm. When the barrier was increased to 167 kJ/mol, probably the highest reasonable value, a rate of $4.5 \times 10^8 \text{ s}^{-1}$ was calculated for 355 nm excitation using 50 cm^{-1} rotor wavenumber, close to the experimentally observed value. For 266 nm excitation, $7.2 \times 10^9 \text{ s}^{-1}$ was obtained, still more than 2 orders of magnitude too fast. Even when an unrealistically low 10 cm^{-1} was employed for the internal rotors, the calculated rates were a factor of 50 higher than the experimental rates at 266 nm.

As an additional control experiment, we recorded the magnitude of the hydrogen signal as a function of the excitation wavelength between 320 and 355 nm. The resulting action spectrum is depicted as an inset in Figure 3. The data points correspond to the signal recorded at a time delay of 100 ns between the two lasers. The H-atom action spectrum matches the UV spectrum of the 3s band of the *tert*-butyl-radical reported in the literature quite well.¹¹ This confirms that the hydrogen atom originates indeed from photodissociation of *tert*-butyl radicals.

(c) Doppler Profiles. Information on the product energy distribution can be obtained from Doppler profiles. Most of the energy released into translation will be carried away by the hydrogen atom on account of momentum conservation, leading to a Doppler broadening of the absorption line. Figure 4 shows the Doppler profile recorded at 266 nm excitation and at a pump–probe delay of 90 ns. The one-color background signal, attributable to hydrogen atoms either produced in the pyrolysis source or by VUV light induced photodissociation was subtracted. The absorption profile is fit well by a Gaussian with a full width at half maximum (fwhm) of 5.6 cm^{-1} , indicating a speed distribution close to Maxwellian. The contributions of the fine structure splitting and the laser bandwidth to the total broadening was neglected. Utilizing the expressions published in the literature,²² we calculated a translational temperature of $9.1 \times 10^3 \text{ K}$ and an expectation value for the translational energy release, $\langle E_T \rangle$, of 113 kJ/mol (27 kcal/mol). This corresponds to 38% of the excess energy released into translation.

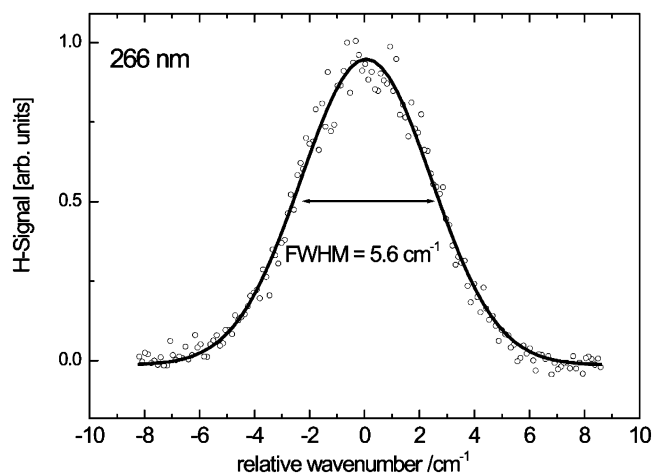


Figure 4. Doppler profile of the hydrogen atom released from *tert*-butyl at 266 nm excitation. The solid line represents a Gaussian fit with a fwhm of 5.6 cm^{-1} . This corresponds to an expectation value of 113 kJ/mol for the translational energy release.

The Doppler profiles obtained upon excitation of the 3s state suffer from a large one-color background signal of roughly 30%, leading to a high noise level after background subtraction that permits only a crude analysis. The profiles show a fwhm of roughly 5 cm^{-1} , corresponding to a translational energy release, $\langle E_T \rangle$, of $90 \pm 20\text{ kJ/mol}$, around 40% of the excess energy. Thus, within the accuracy of the data, the amount of energy released into translation is similar at all wavelengths.

Discussion

It is assumed that electronically excited states of radicals often decay rapidly by internal conversion. In the *tert*-butyl radical this assumption seems to be justified at low excitation energies. The rates observed at excitation energies below 360 kJ/mol (wavelength above 330 nm), corresponding to excess energies below approximately 200 kJ/mol, are well described by simple RRKM calculations. Thus, the photodissociation dynamics can be understood within this rather straightforward picture: After optical excitation into the 3s state, the *tert*-butyl radical decays by internal conversion into the electronic ground state, converting electronic into internal energy. Radicals with an internal excitation equivalent to a vibrational temperature of around 2200 K are formed. The internally hot radicals subsequently dissociate in a way that is appropriately described by statistical theories of chemical reactions. This means that dissociation is the rate-limiting step and that both internal conversion and redistribution of vibrational energy are fast compared to the dissociation. A fast internal conversion is also in agreement with the diffuse and structureless absorption spectrum.

However, the striking feature in the photodissociation of *tert*-butyl is the sudden decrease in the observed rates upon increasing the excitation energy from 360 to 375 kJ/mol, which is difficult to explain. Since the H-atom signal depended linearly on the excitation laser energy and the H-atom action spectrum matches the absorption spectrum of *tert*-butyl, higher-order processes, like dissociative photoionization or photodissociation of the reaction product butene, cannot account for the signal. It is of course possible that the coupling between the initially excited 3s state and the electronic ground state simply becomes less efficient, due to smaller Franck–Condon factors in the corresponding matrix element. It is surprising though that this would lead to such a rather sharp step. Thus, we believe that a competing decay channel becomes available for deactivation of the initially excited state.

At this point, we have to consider possible alternative reaction channels, in particular those associated with initial C–C bond cleavage, on which we gain little information by our experimental method. The thermochemically most relevant reaction channels of *tert*-butyl are summarized in Figure 5. Direct C–C bond cleavage in *tert*-butyl, leading to the formation of dimethylcarbene ($\Delta_f H^\circ = 271\text{ kJ/mol}^{23}$) and a methyl radical, is thermochemically barely possible at our excitation energies. Isomerization to an iso-butyl radical via a [1,2]-H-shift with subsequent loss of methyl and formation of propene provides a more favorable route to C–C bond cleavage. Formation of iso-butyl was indeed observed in matrix isolation studies of *tert*-butyl, but it could not be ruled out that it appeared due to a recombination reaction in the matrix cage.²⁴ The barriers to such hydrogen shifts are not well-known, but for the rearrangement from allyl to 2-propenyl, a barrier of 276 kJ/mol was calculated,⁶ substantially higher than the barrier to H-loss in *tert*-butyl. Thus, C–C bond cleavage is less likely than H-loss in *tert*-butyl. It would be interesting, however, to investigate whether the channel contributes to the photodissociation dynamics. Further H-loss from any of the products of C–C bond cleavage is thermochemically not possible in a one photon process.

Additional insight can be obtained by comparing the results described above with earlier experiments on the ethyl radical.⁹ As mentioned in the Introduction, the rates for H-loss in ethyl obtained upon photoexcitation at energies between 265 and 240 nm were 3–4 orders of magnitude slower than expected from simple RRKM calculations. The translational energy release found in these experiments, consistent with a slow dissociation, was independently confirmed by Rydberg time-of-flight spectroscopy.²⁵ Since the barriers for H-loss are roughly similar, the data obtained for ethyl and *tert*-butyl can be compared with each other. Interestingly, the rate for H-loss in ethyl at 265 nm is on the order of several 10^6 s^{-1} and thus even smaller than in *tert*-butyl at 266 nm, although the higher density of states in *tert*-butyl due to the presence of additional methyl rotors should slow down the dissociation. This shows that dissociation is not the rate-limiting step. It also suggests that this might be a general phenomenon in alkyl radicals. Recent electronic structure calculations on ethyl²⁶ provide a possible explanation. They indicate a crossing between the 3s and the $3p_x$ state at a geometry with an extended C–C bond length, creating a minimum on the potential energy surface of the $3p_x$ state.

The ethyl work leads us to the following speculative explanation of the observation: In our preliminary picture of the dissociation process, at least one of the 3p states has a minimum at a geometry far away from the ground state equilibrium geometry which leads to a longer lifetime of this state than previously thought, maybe due to poor coupling with the electronic ground state. The diffuseness of the absorption spectrum might then be due to the high density of states in the Franck–Condon region. This 3p state might be coupled with the lower-lying 3s-state and provide an efficient means for deactivation of this state. In *tert*-butyl, the coupling occurs at a significant excess energy of roughly 2500 cm^{-1} in the 3s state and is thus not relevant at low excitation energies. In ethyl, on the other hand, efficient coupling might already be present at the bottom of the well of the 3s state. Curve crossings are quite abundant in radicals. For example, a three-state conical intersection between the three 3p-states was recently detected in ethyl, albeit at higher energies.²⁷ Of course the hypothesis outlined here requires further confirmation. As a first step, we want to investigate the H-loss from other alkyl radicals soon, to see

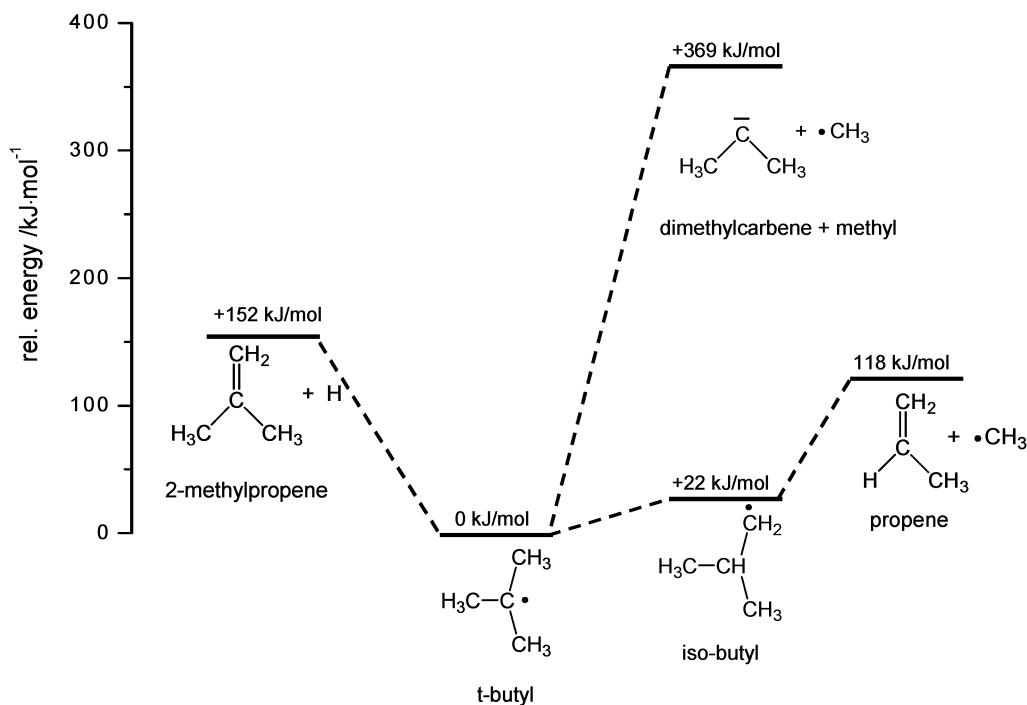


Figure 5. Energy level diagram illustrating the energetically most important reaction channels. The numbers given correspond to the heats of formation relative to *tert*-butyl. Isomerization to iso-butyl seems to provide an energetically favorable route to C–C bond cleavage, but [1,2] H-shifts are associated with considerable barriers.

whether a slow rate is really a general feature in the photodissociation of alkyl radicals.

Often the translational energy distribution yields insight into the photodissociation dynamics. The values of $\langle E_T \rangle$ observed in the experiments on *tert*-butyl are rather high for H-loss reactions described by statistical theories. At 266 nm excitation, around 38% of the excess energy was released into translation. The Doppler profiles recorded at low excitation energy do not have the quality to extract detailed information, but the observed $\langle E_T \rangle$ seems to be on the same order of magnitude. Typically, the translational energy release for hydrogen loss from radicals in a statistical dissociation processes lies around 20% of the excess energy. For comparison, $\langle E_T \rangle = 24\%$ was observed in the unimolecular dissociation of allyl forming allene,⁶ and $\langle E_T \rangle = 22\%$ in the dissociation of propargyl, C_3H_3 , leading to formation of cyclopropenylidene.⁸ In the unimolecular dissociation of ethyl a somewhat larger value of $\langle E_T \rangle = 28\%$ was measured.⁹ Somewhat lower fractions have been measured for H-loss from aromatic molecules.^{15,17,28} A possible reason for a large translational energy release in a slow dissociation process is the existence of a significant reverse barrier (larger than the 6 kJ/mol cited in the Introduction), because this energy is not statistically distributed between the various degrees of freedom, but preferentially released as translation.²⁹

Summary and Conclusion

We investigated the photodissociation dynamics of isolated *tert*-butyl radicals in a molecular beam, generated from azo-*t*-butane by flash pyrolysis. The radicals were optically excited into the 3s state between 355 and 320 nm and the 3p state at 266 nm. The hydrogen atoms formed in the unimolecular dissociation were detected by [1+1'] photoionization. At excitation energies between 355 and 330 nm (335–360 kJ/mol), the dissociation dynamics can be understood in a straightforward picture: The initially excited state decays rapidly by internal conversion, forming internally hot ground-state radicals. These

radicals dissociate in a statistical manner with rates on the order of 10^8 s^{-1} , appropriately described by RRKM theory. At excitation energies above 360 kJ/mol, the dissociation rate drops by an order of magnitude. At this level of excitation, dissociation is not anymore described well by RRKM theory, because dissociation does not seem to be the rate limiting step. Our present hypothesis that has yet to be confirmed is an interaction of the initially excited 3s state with a higher-lying, long-lived 3p state. Direct excitation of the 3p state at 266 nm leads also to a slow dissociation.

Acknowledgment. This work was financially supported by the Deutsche Forschungsgemeinschaft under contract number Fi575/3-1. M.Z. acknowledges a fellowship within the Bioin-formation program of the Fonds der Chemischen Industrie, together with the BMBF (federal ministry of education and research).

References and Notes

- (1) Warnatz, J. in *Combustion Chemistry*; Gardiner, W. C. J., Ed.; Springer: New York, 1984.
- (2) Tsang, W.; Hampson, R. F. *J. Phys. Chem. Ref. Data* **1986**, *15*, 1087.
- (3) NIST webbook, <http://webbook.nist.gov/chemistry/2001>.
- (4) Knyazev, V. D.; Dubinsky, I. A.; Slagle, I. R.; Gutman, D. *J. Phys. Chem.* **1994**, *98*, 5279.
- (5) Deyerl, H.-J.; Gilbert, T.; Fischer, I.; Chen, P. *J. Chem. Phys.* **1997**, *107*, 3329.
- (6) Deyerl, H.-J.; Fischer, I.; Chen, P. *J. Chem. Phys.* **1999**, *110*, 1450.
- (7) Fischer, I.; Chen, P. *J. Phys. Chem. A* **2002**, *106*, 4291.
- (8) Deyerl, H.-J.; Fischer, I.; Chen, P. *J. Chem. Phys.* **1999**, *111*, 3441.
- (9) Gilbert, T.; Grebner, T. L.; Fischer, I.; Chen, P. *J. Chem. Phys.* **1999**, *110*, 5485.
- (10) Fischer, I. *Chimia* **2000**, *54*, 96.
- (11) Wendt, H. R.; Hunziker, H. E. *J. Chem. Phys.* **1984**, *81*, 717.
- (12) Lengsfeld, B. H., III; Siegbahn, P. E. M.; Liu, B. *J. Chem. Phys.* **1984**, *81*, 710.
- (13) Kohn, D. W.; Clauberg, H.; Chen, P. *Rev. Sci. Instrum.* **1992**, *63*, 4003.
- (14) Zacharias, H.; Rottke, H.; Danon, J.; Welge, K.-H. *Opt. Commun.* **1981**, *37*, 15.

- (15) Tsukiyama, K.; Bersohn, R. *J. Chem. Phys.* **1987**, *86*, 745.
- (16) Robin, M. B.; Hart, R. R.; Kuebler, N. A. *J. Am. Chem. Soc.* **1966**, *89*, 1573.
- (17) Park, J.; Bersohn, R.; Oref, I. *J. Chem. Phys.* **1990**, *93*, 5700.
- (18) Pacansky, J.; Koch, W.; Miller, M. D. *J. Am. Chem. Soc.* **1991**, *113*, 317.
- (19) Gilbert, R. G.; Smith, S. C. *Theory of Unimolecular and Recombination Reactions*; Blackwell Scientific: Oxford, U.K., 1990.
- (20) We would like to thank M. Quack for making the program available to us.
- (21) Hase, W. L.; Bunker, D. L. QCPE 209.
- (22) Demtröder, W. *Laser Spectroscopy*; Springer: Berlin, 2002.
- (23) Ford, F.; Yuzawa, T.; Platz, M. S.; Matzinger, S.; Fülcher, M. *J. Am. Chem. Soc.* **1998**, *120*, 4430.
- (24) Pacansky, J.; Chang, J. S.; Brown, D. W. *Tetrahedron* **1982**, *38*, 257.
- (25) Amaral, G.; Xu, K.; Zhang, J. *J. Chem. Phys.* **2001**, *114*, 5164.
- (26) Baumann, H.; Chen, P.; Fischer, I. in preparation.
- (27) Matsika, S.; Yarkony, D. R. *J. Chem. Phys.* **2002**, *117*, 6907.
- (28) Satyapal, S.; Johnston, G. W.; Bersohn, R.; Oref, I. *J. Chem. Phys.* **1990**, *93*, 6398.
- (29) Mordaunt, D. H.; Osborn, D. L.; Neumark, D. M. *J. Chem. Phys.* **1998**, *108*, 2448.